One Dimensional Melting in Single-Screw Extruders

One Dimensional Melting in Single-Screw Extruders

Gregory A. Campbell, Castle Research Associates, Jonesport, ME
Mark A. Spalding, The Dow Chemical Company, Midland, MI

Abstract

For special operating conditions and resins, the melting process for single-screw extruders can occur via a very non-traditional mechanism. For this process, melting occurs almost exclusively at the solid bed-melt film interface between the solid bed and the barrel wall. The newly molten material then infiltrates the solid bed such that a melt pool does not form on the pushing side of the channel. This paper describes the mechanism and provides a model for the melting process.

Introduction

Melting inside single-screw extruders typically occurs at all four edges of the solid bed with the majority of the melting occurring at the solid bed-melt film interface located between the solid bed and the barrel wall. The newly molten resin from this location is then conveyed by the motion of the screw to a melt pool located at the pushing side of the channel. A photograph that shows this process via a Maddock solidification experiment is provided in Figure 1. This melting process occurs in the majority of single-screw extrusion operations, and it melts the resin at relatively high rates.
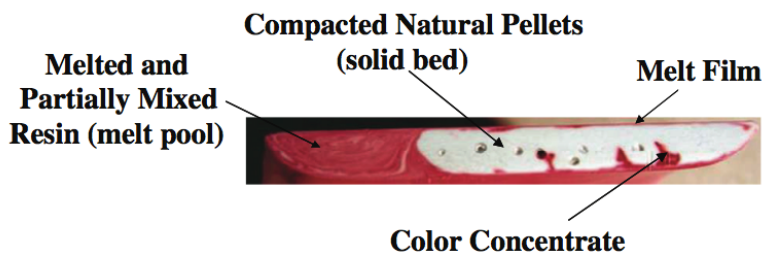

Figure 1. Photograph of resin solidified in the transition section after a Maddock solidification experiment.

For very special and sometimes unpredictable conditions, the melting process can occur by a different mechanism. Here, the melting is occurring predominately at solid bed-melt film interface located between the solid bed and barrel wall. The newly molten resin infiltrates the solid bed by flowing between the solid resin particles. A photograph of a cross section is shown by Figure 2. This cross section was for a specialty powder resin at a location about 3 diameters downstream from the start of the transition section. The pressure in the screw channels was very low and the screw rotation rate was 30 rpm. The melting rate and extrusion rate were very low, and the melt film between the solid bed and barrel wall was considerably thicker than that for the conventional melting process. The grainy cross section shown in Figure 2 is due to a mixture of molten and solid particles at the time of the Maddock solidification experiment. As melting progresses in the downstream direction, the bulk temperature of the channel increased, the level of solids decreased, and the cross sectional view became less grainy in appearance.

Pushing Side   Trailing Side

Figure 2. Photograph of a specialty powder resin that is melting via the one dimensional melting mechanism. Even at this early location in the melting process, the thickness of the melt film adjacent to the barrel wall was thicker than normal.

In this paper we address the phenomena of poor melting due to one dimensional melting (or top down melting) as shown by Figure 2. This process is often observed when extruding powders or very low viscosity polymer pellets at conditions when the pressure in the channel is very low. In order to understand the difference between this melting problem and conventional melting, a review of the development of single-screw melting theory follows. Then the differences between the conventional melting theory and one dimensional melting will be developed. The model presented here compliments previously defined models for melting in conventional channels [1] and melting in barrier screw sections [2].

Conventional Melting Process

Experiments for studying the single-screw extrusion melting mechanism were first carried out by Maddock [3] and then by Street [4]. The melting mechanism was observed by performing Maddock solidification experiments. For these experiments, the extruder was fed with a mixture of natural and colored (1-3%) polymer. When steady state was achieved, screw rotation was stopped, and full cooling was applied to the barrel, solidifying the polymer in the channels. Usually, the original conditions existing in the extruder were retained.

By examining the cross sections of the solidified polymer after taking it out of the screw channel, a clear picture of the melting behavior was obtained, as shown in Figure 1. Their famous solidification experiments revealed that melting in many situations takes place in a specific order. The experiments showed that after melting began, there was a continuous solid bed and a melt film over the inner barrel surface. Later the solid bed was completely surrounded by melt. Farther downstream, a melt pool developed between the pushing flight and the solid bed. The solid bed disappeared gradually all the way down the channel [3].

Tadmor's research group [5,6] observed similar melting phenomena. They studied many different materials which included low density polyethylene (LDPE), high density polyethylene (HDPE), acrylonitrile butadiene styrene (ABS), rigid polyvinyl chloride (PVC), and polypropylene (PP) resins using different operating conditions and extruder geometries. The results were interpreted to demonstrate that the Maddock melting mechanism prevails in quite a large range of melting processes with most resins. Other investigators' experiments led to other melting phenomena, such as the acceleration of the solid bed, break up of the solid bed, and a melt pool existing by the trailing flight [7]. Maddock first proposed the physical description of the melting process in 1959. In his description, the energy for the melting process came from two sources: energy conduction from the barrel, and viscous dissipation from the film at the inner barrel surface. Beginning from 1966 when Tadmor [8] set up the first mathematical model based on the Maddock melting mechanism, he proposed a reorganizing solid bed that led to a focus on the x-dimension as rate controlling in the melting process. That is, the rate of melting was defined as the ratio of the solid bed width to the width of the channel.

The classical melting data originally presented by Tadmor and Klein [6] for PE resin was examined using digital dimensional analysis [10] and the melting results for three specific runs are shown Figure 3.

For essentially all of the data sets found in Tadmor and Klein [6] the melting results resemble the data shown in Figure 3. The data analysis is of course most difficult near the end of melting, and in essentially all cases the fraction of the bed remaining in the cross-channel direction is much greater than in the thickness direction. Also, in general the last third of the x direction material appears to melt in the last turn of the channel, creating nearly a step function in the melting rate with respect to the axial distance, as shown in Figure 2. Step functions, however, do not in general occur in processes that are heat conduction dominated. To reiterate, the digital analysis conclusively demonstrated that the y direction thickness always goes to zero before the x direction width [9,10]. This observation led us to the development of a new physical model that is based on these new observations. It is interesting to note that Lindt recognized this melting behavior experimentally for polypropylene (PP) resin in 1976 [11].
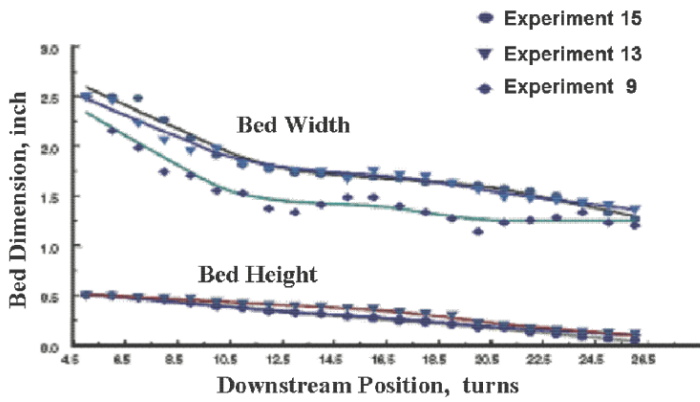
Figure 3. Melting data from Tadmor for PE resins [6,10]. At a downstream position of 25 turns, the solids were completely melted and thus the bed width and bed height were zero.

Theory Development

The new single-screw melting concept was presented in 2009 [1] for the conventional melting process. The new model predicted that the solid bed melted due to dissipation and heat transfer in all four melt films surrounding the melting solid bed, as shown in Figure 4.
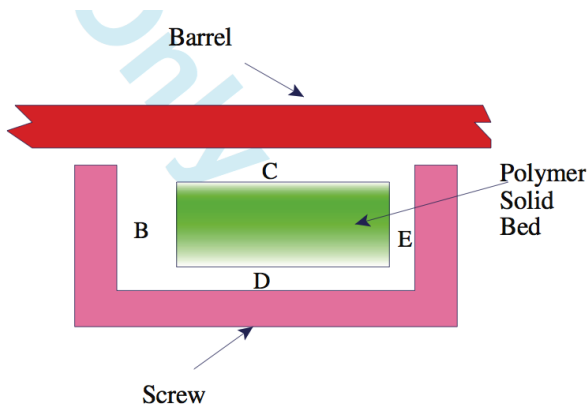

Figure 4. Schematic for the zones of the new melting concept.

Consistent with the results presented in Figure 3, separate melting dynamics were defined for the four melt films depicted in Figure 4; C is the film between the solid bed and the barrel wall, D is the film at the screw root (or core) polymer interface, E is the film at the trailing flight of the screw, and B is the film (or melt pool) on the pushing side of the screw flight.

Previous analysis of dissipation in extrusion [12] over predicted the polymer melt temperature when barrel rotation dissipation was used. We therefore use the screw rotation velocities in this analysis because the process is dissipation dominated [13-18] and dissipation is not frame indifferent. We start with the analysis developed by Tadmor and Klein [6]. The diagram for the new adaptation of the Tadmor analysis is shown in Figure 5. We start by unwrapping the screw into the x, y, and z coordinates. The velocity gradient in the z direction goes from V_{sz}, the solid bed velocity in the downstream directions (z direction), to 0 at the barrel interface. A similar diagram was developed for the other three fluid interfaces around the solid bed, remembering that for these liquid interfaces the metal velocity is the screw velocity, as shown in Figure 6.

We retain V_{sy} as a variable because this allows us to calculate the change in bed thickness in our re-analysis of the literature data, as shown in Figure 3. The nomenclature used here follows that used by Tadmor and Klein [6] as much as possible. Where deviations occur, a full explanation will be presented. A nomenclature list is presented at the end of the paper. The velocity of the solid bed in the z direction, V_{sz}, is as defined by Tadmor and Klein. The velocity of the solid bed in the x direction, V_{sx}, due to screw rotation is as follows:

$$V_{sx} = \frac{N\pi D}{60}\sin\theta \qquad (1)$$

$$\tan\theta = \frac{\pi L}{D} \qquad (2)$$

where N is the screw rotation speed in rpm, D is the diameter at the surface of the solid bed, theta is the helix angle at diameter D, and L is the lead length of the flight.

We calculated the thickness of the melt film, $?_c$, at film C using similar assumptions used by Tadmor and Klein [6] and thus solve their Equation (5-23) for $V_{sy,C}$, the velocity of the loss of the solid bed due to melting at ?c.

$$V_{sy,C} = \frac{\left[\dfrac{k_m}{\delta_c}(T_b - T_m) + \dfrac{\mu V_j^2}{2\delta_c}\right]}{\rho_s\lambda + \left[\rho_s c_s(T_m - T_s)\right]} \qquad (3)$$

where k_m is the thermal conductivity of the melt, T_b is the barrel temperature, T_m is the melting temperature of the resin, micro is the shear viscosity, V_j is the vectorial velocity in the film (discussed later), ρ_s is the density of the compacted solid bed, lamda is the heat of fusion, c_s is the heat capacity, and T_s is the temperature of the solid bed. The term $V_{sy,C}$ here is equivalent to Tadmor and Klein's V_{sy}. Equation (3) is simply an energy balance for the melting process [1]. Melting velocities at the other three interfaces $V_{sy,D}$, $V_{sx,B}$, and $V_{sx,E}$ are essentially identical to that for Equation (3) except that the vectorial velocity used corresponds to the specific film. These equations were omitted here.
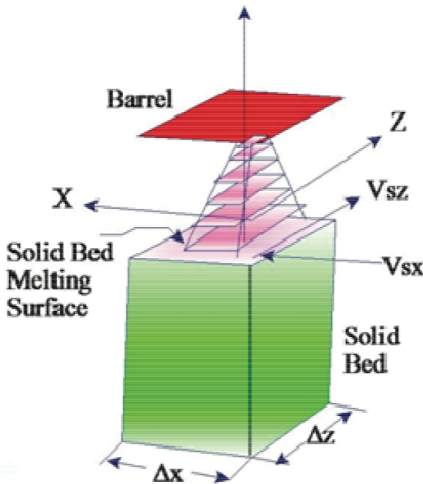

Figure 5. Melting differential element for a rotating screw for the melt film in zone C.

The melting velocities of the solid bed interfaces are the foundation of this new approach. The mathematical equality to calculate the rate of loss of the solid at the interface next to the barrel is found in Equation (4).

$$\left.\frac{dY}{dt}\right|_{\&} = V_{sy,C} \qquad (4)$$

where Y is the local thickness of the solid bed and t is the independent time variable.

The melt film thickness for zone C, ?, is determined using Equation (5). Note that V_{sx} is essentially numerically equal to the traditional V_{bx} as specified by Tadmor and Klein because of the small value of the film thickness.

$$\delta_c = \left\{ \frac{\left[\left[2k_m(T_b - T_m) + \mu N_j^2\right] X / \alpha\right]}{V_{sx} \rho_m \left[c_s(T_m - T_s) + \lambda\right]} \right\}^{\frac{1}{2}} \qquad (5)$$

where X is the local width of the solid bed and α is a fitting factor. Equation (5) is a mass balance for the zone C film and is essentially identical to Tadmor and Klein's [6] Equation (5-31). The flow equation is a first-order approximation since it neglects flows due to pressure gradients. Ideally, the value of α is set to 2 so as to provide an average thickness for the film in the crosschannel direction. The value of α was set to 0.5 for the simulation here to force the melting lengths to be equivalent to those in the literature.

The film thickness, δ_e, for zone E was determined using a similar mass balance equation as follows:

$$\delta_e = \left\{ \frac{\left[\left[2k_m(T_b - T_m) + \mu N_j^2\right] Z / \alpha\right]}{V_{sz} \rho_m \left[c_s(T_m - T_s) + \lambda\right]} \right\}^{\frac{1}{2}} \qquad (6)$$

where Z is downstream position of the solid bed. The melt film thicknesses, δ_b and δ_d for zones B and D were found by difference:

$$\delta_b = W - X - \delta_e \qquad (7)$$

$$\delta_d = H - Y - \delta_c \qquad (8)$$

where W is the width of screw channel and H is the local depth of channel.

The boundary conditions for the velocity at the screw root interfaces are shown in Figure 6.

The results of this analysis can be found in a previous paper [1] and are referred to here as the new melting model.

One-Dimensional Melting Model

The problem at hand has different dissipation physics. In this case the solid bed is conceptualized as depicted in Figure 7.

Comparing Figure 7 to Figure 4 it is observed that melting zones B, D, and E are no longer available for producing dissipation to aid the melting. There is some free space around the solid which allowed the solid to be pushed up the transition. However this space is not wide enough to allow the fluid at the top of the bed to encapsulate the bed. Thus the expressions for δ_D, δ_B, and δ_E now reduce to zero. Also the thickness of the film in C, where we have previously demonstrated that it produces the greatest melting flux [1], will now not just be modeled as the Tadmor model for δ_c via Equation 5. In this analysis the initial film thickness is defined the same as for our new melting model; i.e., Equation 5. Then as the solid bed melts at the barrel interface the δ_c becomes a function of the channel thickness and the solid bed remaining.
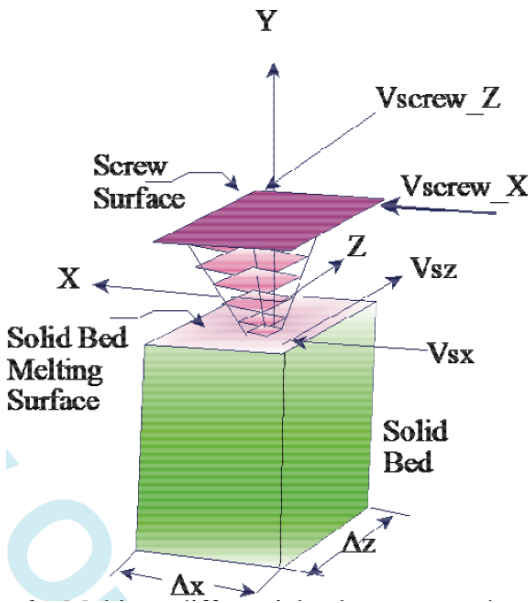
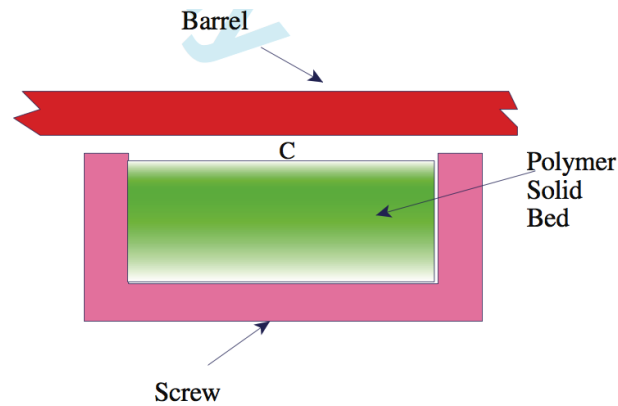Figure 6. Melting differential element at the screw surfaces for a rotating screw reference frame.

Figure 7. Conceptual melting physics for one dimensional melting.

$$\delta_{C\_melt} = H_0 - A_z Z - Y(Z) \qquad (9)$$

where the film thickness in now $?_{C\_melt}$ once the melting starts. Here H_0 is the initial channel thickness, A_z is the rate that the channel decreases in depth with the down channel distance Z, and $Y(Z)$ is the bed thickness at any Z.

This increase in film thickness at the barrel solid bed interface decreases the dissipation because the local shear rate decrease as the film thickness increases. It will be found that this caused the bed to melt much more slowly.

Results and Discussion

We are now in a position to determine if the proposed theory will produce results that are consistent with reported observations that these types of materials melt more slowly because the bed has not been encapsulated.

This new theory requires the solution of only two coupled differential equations, unlike the model presented in 2009 where there are five simultaneously coupled equations. Here x, y, and z are the local coordinates of the solid bed:

$$\left.\frac{dY}{dt}\right|_{\delta_{C\_melt}} = V_{sy,C} \qquad (10)$$

$$\frac{dZ}{dt} = V_{sz} \qquad (11)$$

We used a differential equation solver to obtain the results of the initial value problem.

Typical simulation results are presented in Figure 8 for the conventional melting model with melting in all four melt films, C, D, E, and B. As shown by this figure, the Y thickness goes to zero at a down channel position of 220 cm into the melting section. It is seen that the change in the thickness (x direction) leaves about 60% of the original bed width remaining just at the end of melting. The end of melting is defined as when the y direction thickness of the solid bed goes to zero and thus the x direction thickness also goes to zero because there is no more material to melt. This simulation was performed using a PE resin with a shear viscosity of 880 Pa-s.

Using the same PE resin with the same physical properties, the model was modified to represent the melting physics shown in Figure 7. The results are presented in Figure 9. It is observed that the bed width remains constant because there is no dissipation at the screw helix wall, zones B and E in the new model physics, as shown in Figure 4. For the one dimensional melting from the barrel surface, unlike the results in Figure 8 where the bed thickness was consumed at a down channel position of about 220 cm, about 25% of the original bed remains.
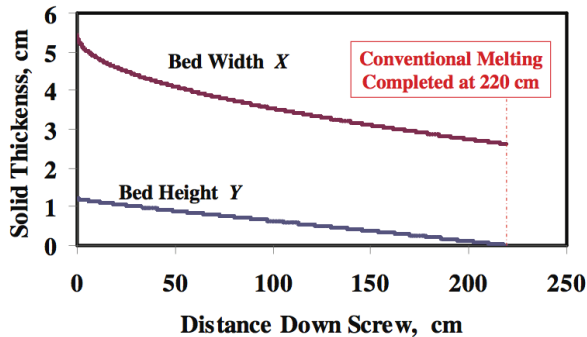

Figure 8. Simulation results using the new melting model [1] for the conventional melting process; i.e., melting is occurring in all four melt films.
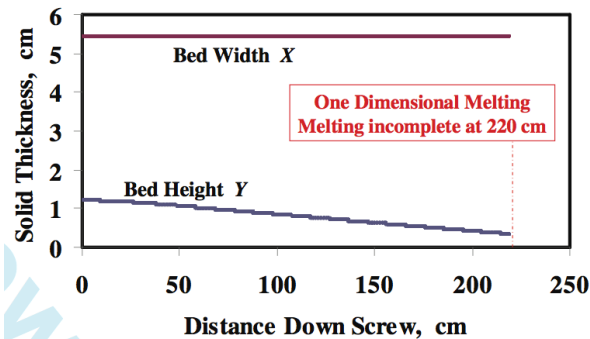

Figure 9. Simulation results for melting only from the barrel surface; i.e., one dimensional melting. About 75% of the resin was melted at end of the transition section.

One dimensional melting and melt infiltration into the solid bed will reduce the melting capacity of the process, as shown by Figure 9. The melting mechanism can switch from the normal conventional melting to the poor melting performance shown above due to the lack of pressure in the melting channel. Pressure in the channel is needed to compact the solid polymer feedstock [19] into a nonporous bed, eliminating the possibility of melt infiltration. Melting rates are also known to increase with increasing pressure in the channel [20]. Moreover, as the melt film between the barrel and solid bed becomes thicker in the downstream direction, energy dissipation and the melting rate will be reduced. With reduced energy dissipation, the effect of energy conduction becomes more important.

Conclusions

A new approach has been developed that correlates with observations of several polymer systems that do not melt in the conventional manner. The new alternative model proposed for the melting of the solid polymer bed in a single-screw extruder has been modified to analyze the melting phenomena of a solid bed in a single location and allows the infiltration of molten resin into a porous solid bed. The model alters the heat transfer and melting velocities proposed in our previous paper where a new melting concept was modeled [10]. This modeling effort demonstrates that as the melt film increases at the barrel solid interface the dissipation decreased due to lower shear rate and the bed melts much slower.

Nomenclature

c_s heat capacity of the solid.
D diameter at the surface of the solid bed.
H local channel depth.
k_m thermal conductivity of the melt.
L lead length of the flight.
N screw rotation speed in rpm.
t independent time variable.
T_b barrel temperature.
T_m melting temperature of the resin.
T_s temperature of the solid bed.
V_j vectorial velocity in the films.
V_{bx} velocity of the barrel in the x direction for a barrel rotation reference frame (not used).
V_{sx} velocity of the solid bed in the x direction.
V_{sy} velocity of the solid bed consumption in the thickness direction at the zone C film (Tadmor).
$V_{sy,C}$ velocity of the solid bed consumption in the thickness direction at the zone C interface (y direction).
V_{sz} velocity of the solid bed in the z direction.
W width of the channel perpendicular to the flight.
X width of the solid bed.
x independent variable in the cross-channel direction.
Y thickness of the solid bed in the y direction.
y independent variable in the channel-depth direction.
Z downstream position of the solid bed.
z independent variable in the down-channel direction.
α fitting factor.
theta helix angle at diameter D.
ρ_m density of the molten polymer.
ρ_s density of the compacted solid bed.
λ heat of fusion.
$?_b$ thickness of melt film B.
$?_c$ thickness of melt film C.
$?_{c\_melt}$ thickness of melt film C 1 D melting.
$?_d$ thickness of melt film D.
$?_e$ thickness of melt film E.
μ shear viscosity.

Acknowledgments

References

1. G.A Campbell, M.A. Spalding, and Z. Tang, SPEANTEC Tech. Papers, 55, 147 (2009).
2. G.A. Campbell and M.A. Spalding, SPE-ANTEC Tech. Papers, 56, 418 (2010).
3. B.H. Maddock, SPE J., 15, 383 (1959).
4. L.F. Street, Int. Plast. Eng., 1, 289 (1961).
5. Z. Tadmor, I.J. Duvdevani, and I. Klein, Polym. Eng. Sci., 7, 198 (1967).
6. Z. Tadmor and I. Klein, "Engineering Principles of Plasticating Extrusion," Robert E. Krieger publishing company, New York, 1978.
7. F. Agassant, P. Avenas, P.J. Carreau, and J.Ph. Sergent, and "Polymer Processing: Principles and Modeling," Oxford University Press, New York 1991.
8. Z. Tadmor, Polym. Eng. Sci., 6,185(1966).
9. G.A. Campbell, Z. Tang, C. Wang, and M. Bullwinkel, SPE-ANTEC Tech. Papers, 49, 213 (2003).
10. G.A. Campbell and Z. Tang, SPE-ANTEC Tech. Papers, 50, 162 (2004).

11. J.T. Lindt, Polym. Eng. Sci., 16, 284 (1976).
12. G.A. Campbell and N. Dontula, Intern. Polym. Process., 10, 30 (1995).
13. G.A. Campbell, M.A. Spalding, and F. Carlson, SPEANTEC Tech. Papers, 54, 267 (2008).
14. G.A. Campbell, P.A. Sweeney, and J.N. Felton, Polym. Eng. Sci., 32, 1765 (1992).
15. G.A. Campbell, P.A. Sweeney, and J.N. Felton, Intern. Polym. Proc., 7, 240 (1992).
16. G.A. Campbell, P. A. Sweeney, N. Dontula, and C. Wang, Intern. Polym. Proc., 11, 3 (1996).
17. G.A. Campbell, H. Cheng, C. Wang, M. Bullwinkel, and M. A. te-Riele, SPE-ANTEC Tech, Papers, 47,152 (2001).
18. G.A. Campbell, C. Wang, H. Cheng, M. Bullwinkel, M.A. te-Riele, Intern. Polym. Proc., 16, 323 (2001).
19. K.S. Hyun and M.A. Spalding, Polym. Eng. Sci., 30, 571 (1990).
20. M.A. Spalding, K.S. Hyun, and B.R. Cohen, SPEANTEC Tech. Papers, 43, 202 (1997).

Key Words: Extrusion, Melting, Single-Screw, Mechanism, Theory, Modeling.

Return to .